

Room temperature superconductivity in ScH₁₂ with quasi-atomic hydrogen below megabar pressure

Qiwen Jiang^a, Defang Duan^{a,*}, Hao Song^b, Zihan Zhang^a, Zihao Huo^a, Tian Cui^{b,a,*},

Yansun Yao^c

^a *State Key Laboratory of Superhard Materials, College of Physics, Jilin University, Changchun 130012, China*

^b *Institute of High Pressure Physics, School of Physical Science and Technology, Ningbo University, Ningbo, 315211, People's Republic of China*

^c *Department of Physics and Engineering Physics, University of Saskatchewan, Saskatoon, Saskatchewan S7N 5E2, Canada*

* Corresponding author: duandf@jlu.edu.cn (Defang Duan), cuitian@nbu.edu.cn (Tian Cui)

Abstract

Achieving superconductivity at room temperature is a century-old dream in the field of physics and materials. Recent discoveries on high- T_c superconductivity in H_3S and LaH_{10} at high pressure have directed the search for room temperature superconductors to compressed hydrides with conventional phonon-mediated superconductivity. Here, we predict an exceptional superhydride ScH_{12} which has potential room-temperature superconductivity with a calculated T_c of 313 K at pressures below one megabar. In contrast to H_3S and LaH_{10} , the sublattice of hydrogen in ScH_{12} is arranged as quasi-atomic peanut-like units. The emergence of high T_c is attributed to the van Hove singularities and high phonon frequencies of quasi-atomic hydrogen. This distinct structure is also found in MgH_{12} , ZrH_{12} , HfH_{12} and LuH_{12} , all of which are room temperature superconductors with the calculated T_c above 300 K. This work provides innovative direction to experimental search for room temperature superconductors.

It was predicted that hydrogen molecules (H_2) in solid hydrogen would dissociate into atomic form under extreme compression, which causes the solid hydrogen to become metallic. From theoretical perspective, metallic hydrogen has all ingredients needed for a room temperature superconductor, *i.e.*, high-frequency phonons, high density of states (DOS) at the Fermi level, and very strong electron-phonon coupling^{1,2}. However, the direct compression of solid hydrogen may require a pressure in excess of 500 GPa^{3,4} to reach a metallic state and this poses an extreme difficulty in experiments. Alternatively, highly compressed hydrides were predicted to become metallic and high- T_c superconductors at much lower pressure than thought to be required for pure hydrogen⁵. In these hydrides, the hydrogen species are ‘precompressed’ by the metal elements and therefore the charge density sufficient for metallization can be achieved at less physical compression^{6,7}.

The diatomic H_2 is a ubiquitous building block of solid hydrogen (e.g., phase I, II, III⁸⁻¹⁰) and of many hydrides as well⁶. According to our survey, at least 70 crystal structures of binary hydrides contain H_2 molecular units, such as $SiH_4(H_2)_2$ ¹¹ and TeH_4 ¹². These ‘molecular’ hydrides usually have moderate superconductivity with a T_c less than 120 K. To increase the T_c in hydrides, one needs to ‘free’ the electrons from their locked positions in the H-H bonds, that is, to weaken the H_2 units toward atomic hydrogen. Along this approach, two prototypic hydrides consist of atomic hydrogen sublattices, the cubic H_3S ¹³⁻¹⁶ and cagelike LaH_{10} ¹⁷⁻²², were predicted to have much higher T_c (in 200-260 K range), which were subsequently confirmed by experiments. Thus, weakening or atomizing H_2 molecule should be considered as a prerequisite for realizing room temperature superconductivity in hydrides.

A tradeoff for a higher electron mobility is the stability -- high T_c hydrides are usually metastable phases due to the less stable hydrogen species. For example, the predicted T_c in metastable YH_{10} ^{17,18}, HfH_{10} ²³ and Li_2MgH_{16} ²⁴ are higher than 200 K. Li_2MgH_{16} , in particular, has the highest predicted T_c up to 473 K. Previous studies suggest that the conventional threshold for semi-stable (likely to be synthesized) compounds is within 50 meV/atom above the convex hull²⁵. Metastable hydrides have been synthesized in

this range, such as PrH_9 (19 meV/atom above the convex hull)²⁶, Ca_2H_5 (20 meV/atom above the convex hull)²⁷, etc. High temperature is a common tool to access and synthesize metastable structures.

In the present work, we focus on metastable hydrogen-rich compounds that are potentially high- T_c superconductors and uncovered a new class of dodecahydrides MH_{12} ($\text{M} = \text{Sc}, \text{Mg}, \text{Zr}, \text{Hf}, \text{Lu}$) with extraordinary T_c higher than room temperature. Different from previously reported atomic (H_3S), cage (LaH_{10}), and planar (HfH_{10}) forms, hydrogen atoms in MH_{12} are regularly arranged in quasi-atomic peanut-like units. All dodecahydrides in this study are predicted to be potential room-temperature superconductors with T_c up to 313-398 K estimated by solving Eliashberg equations. In particular, ScH_{12} is the first room temperature hydride superconductor hitherto predicted at pressures below 100 GPa. Our research provides a promising approach for exploring phonon-mediated high- T_c superconductivity that meets or surpasses the atomic metallic hydrogen.

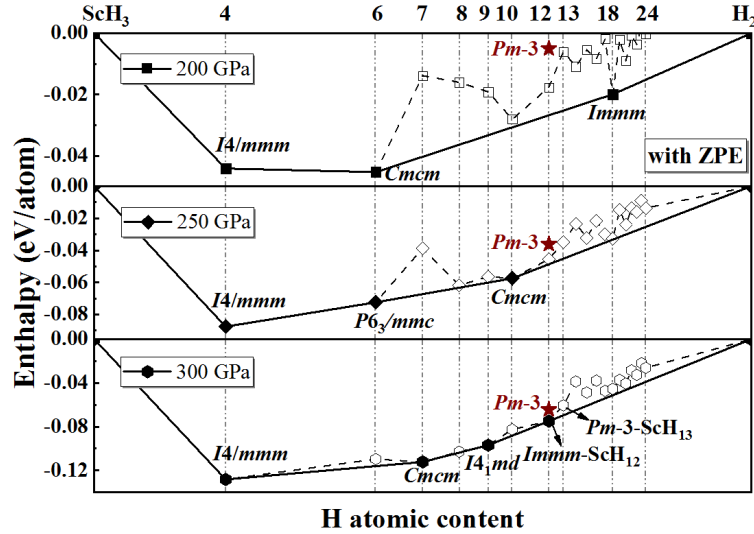


Fig. 1. The thermodynamic convex hull diagram of Sc-H system with respect to starting materials (ScH_3 and H_2) at 200, 250 and 300 GPa. Zero-point energy (ZPE) is included in the calculation. The compositions on the solid line are thermodynamically stable at the corresponding pressure, while those on dashed lines are thermodynamically unstable with respect to other hydrides and H_2 , but they may be dynamically stable. The star near the convex hull represents the metastable $Pm\bar{3}$ phase of ScH_{12} .

We performed variable composition structural searches for Sc-H system in unit cells with up to 24 H atoms in the pressure range of 200-300 GPa using AIRSS code²⁸. The formation enthalpies for the best structures in all considered Sc-H stoichiometries are depicted in the convex hull diagram as shown in Fig. 1 and Fig. S1 of supplemental material. Zero-point energy (ZPE) was included in the enthalpy calculation to account the quantum effects. In this search, we successfully recovered the previously predicted *I4/mmm*-ScH₄, *Cmcm* and *P6₃/mmc*-ScH₆, *Cmcm*-ScH₇, *I4₁md*-ScH₉, *P6₃/mmc* and *Cmcm*-ScH₁₀, *Immm*-ScH₁₂ structures²⁹. Moreover, we found a new hydride *Immm*-ScH₁₈ that lies on the convex hull at 200 GPa. The *Immm*-ScH₁₈ contains molecular H₂ and hydrogen chains as shown in Fig. S2 (optimized lattice parameters are listed in Table S1). Due to the covalence of H₂ molecules, this structure has low electronic DOS at the Fermi level (Fig. S3), and therefore it is unlikely to retain high T_c superconductivity -- we will not discuss it further. On the other hand, two new hydrides ScH₁₂ and ScH₁₃ with unique $Pm\bar{3}$ symmetry appeal our attention. Even though both structures lie slightly above the convex hull (~9 and 7 meV/atom) at 300 GPa, once temperature effects are included via quasi-harmonic free-energy calculations, the $Pm\bar{3}$ phase of ScH₁₂ becomes more stable than the ground state *Immm* at temperatures >1700 K (Fig. S4). This indicates that the $Pm\bar{3}$ phase may be synthesized under high temperature and high pressure conditions.

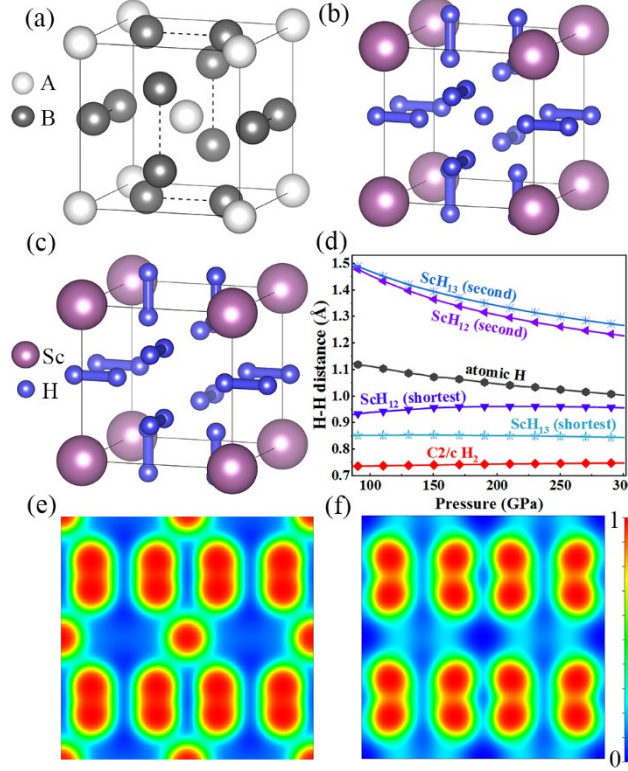


Fig. 2. Crystal structure and bonding properties. (a) The $A15$ type structure (AB_3 , $Pm\bar{3}n$). Crystal structure of (b) ScH_{13} and (c) ScH_{12} . (d) H-H distances in ScH_{12} and ScH_{13} compared to the values in atomic hydrogen solid and molecular hydrogen solid ($C2/c$) at different pressures. ELF of (e) ScH_{13} and (f) ScH_{12} mapped on the (0 0 2) plane.

As displayed in Fig. 2, the structures of $Pm\bar{3}$ - ScH_{12} and $Pm\bar{3}$ - ScH_{13} are variants of the $A15$ type (AB_3 , $Pm\bar{3}n$), with Sc and diatomic H_2 being the two bases. In the $A15$ structure, one base occupies the corners and centers of the cubic lattice, and the other base occupies six planes of the cube (see Fig. 2a). The $Pm\bar{3}$ - ScH_{13} is viewed as Sc atoms forming a cubic lattice with a single H atom occupying the center, and a pair of H_2 units perpendicular to and intersecting each face of the cube (Fig. 2b). If the centered H atom is removed, the structure will turn into the $Pm\bar{3}$ - ScH_{12} structure (Fig. 2c). Interestingly, the $A15$ structure has been known to exist in conventional superconductors, such as Nb_3Sn and Nb_3Ge ³⁰. There are also $A15$ type superconductors in metal hydrides. For example, GaH_3 and GeH_3 have high T_c of 123 K at 120 GPa³¹ and 140 K at 180 GPa³², respectively. Ternary hydride $LiPH_6$ ³³ also adopts the $A15$ -like configuration, which is predicted to be a high- T_c superconductor as well (150-167 K at

200 GPa).

The bonding characteristics of ScH_{12} and ScH_{13} are investigated using electron localization function (ELF), crystal orbital Hamiltonian population (COHP) and Bader charge analysis. Bader analysis (Table S2) reveals significant charge transfer between Sc and H atoms. At 300 GPa, each Sc atom in ScH_{12} and ScH_{13} loses about 1.140 and 1.174 e^- to the surrounding H atoms, respectively. In ScH_{12} , each H_2 pair accepts 0.190 e^- . In ScH_{13} , each H_2 pair accept 0.164 e^- while the isolated H atom accepts significantly more electrons, 0.192 e^- . Since the electrons acquired by hydrogen must populate its antibonding states, this weakens the H-H bonds. In Fig. 2d, we compare the nearest H-H distances (as in H_2 units) of ScH_{12} and ScH_{13} to those in atomic H and molecular H_2 solids. Clearly, both H-H contacts in ScH_{12} and ScH_{13} are longer than the covalent bond length in molecular H_2 , as one would expect for weakened bonds. The on average shorter H-H bonds in ScH_{13} than in ScH_{12} are consistent to the lesser number of electrons in the antibonding orbitals. Interestingly, similar to molecular H_2 , the H-H contact in ScH_{13} does not change with pressure, indicating that the latter still contain molecular H_2 , albeit weaker in strength. We thus term the H_2 unit in ScH_{13} as ‘quasi molecular’. On the other hand, the H-H contact in ScH_{12} keeps increasing at higher pressure, showing a clear tendency of molecular dissociation of H_2 , and reaches almost the same value as that in atomic hydrogen (only 0.05 Å apart) at 300 GPa. Hence, it seems reasonable to refer to the H_2 unit in ScH_{12} as ‘quasi atomic’. The electron clouds surrounding quasi-atomic H_2 are shaped like peanuts, with a high ELF value of ~ 0.84 (Fig. 2f, Fig. S5). The calculated ICOHP values within the H_2 units (Fig. S6) are -3.23 eV in ScH_{12} and -4.91 eV in ScH_{13} , indicating a much stronger bonding interaction in the latter. The ICOHP values between the H_2 units are -0.91 eV in ScH_{12} and -0.55 eV in ScH_{13} . This manifests a stronger inter-molecular interaction in ScH_{12} which causes the weakening of the H_2 units. Although there is no visible electron localization, weak interaction does present between adjacent H_2 units in ScH_{12} , which makes the vibration of the H_2 units collective and therefore promote the superconductivity.

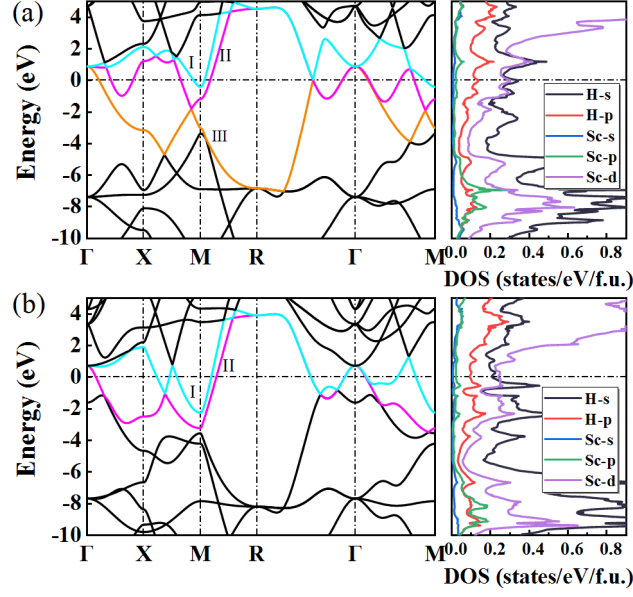


Fig. 3. Electronic band structure and DOS. Electronic band structure and partial DOS for (a) ScH₁₂ and (b) ScH₁₃ at 300 GPa. The bands crossing the Fermi level are labelled I, II, and III.

The electronic band structure and DOS of ScH₁₂ and ScH₁₃ are shown in Fig. 3. Remarkably, a sharp DOS peak is present at the Fermi level in ScH₁₂, corresponding to a van Hove singularity. The total DOS value at the Fermi level (N_{Ef}) is 0.99 states/eV/f.u.. On the other hand, in ScH₁₃ the additional electron raises the Fermi level to above the peak, resulting in a much smaller N_{Ef} (0.69 states/eV/f.u.). In Fig. S7, the N_{Ef} values of ScH₁₂ and ScH₁₃ are compared with the N_{Ef} values of high- T_c hydrides H₃S and LaH₁₀ at 300 GPa. The comparison shows that ScH₁₂ has a significant larger N_{Ef} than others, with a general trend ScH₁₂ > LaH₁₀ > ScH₁₃ > H₃S. High electronic DOS at the Fermi level, in particular those induced by hydrogen, sets a favorable condition for strong electron-phonon coupling (EPC) and superconductivity. For the electronic bands crossing the Fermi level in ScH₁₂, bands I and III possess electron and hole pockets at points M and Γ , respectively. Band II has complex Fermi surface structure including both electron-like and hole-like features.

To examine the dynamical stability of ScH₁₂ and ScH₁₃, we calculated their phonon spectra in the pressure range between 80 and 300 GPa (Fig. 4 and Figs. S8-S9). There are no imaginary phonon frequencies for ScH₁₂ at 90 GPa and above, and for ScH₁₃ at

80 GPa and above, which establish their dynamic stability ranges. It should be noted that the vibrational bands of hydrogen in ScH₁₂ are mixed and dispersive, with all frequencies below 2300 cm⁻¹ (Fig. 4), which is consistent with the disappearance of molecular H₂. For ScH₁₃, the high frequency vibrations still form an isolated non-dispersive block, with the highest frequency around 3000 cm⁻¹, which corresponds to the vibrations of quasi-molecular H₂. For pure molecular hydrogen *C2/c* phase³⁴, the highest vibrational frequency is around 4000 cm⁻¹ at 250 GPa. The lower vibrational frequencies in hydrides indicate weaker H-H bonds induced by interaction between H and metal atoms.

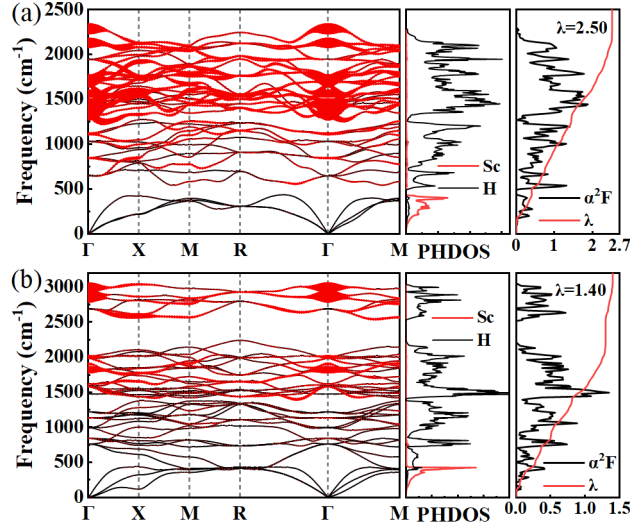


Fig. 4. Phonon and Eliashberg spectral function. Phonon band structure (left), PHDOS (middle), and Eliashberg spectral function $\alpha^2F(\omega)$ (right) for (a) ScH₁₂ and (b) ScH₁₃ at 300 GPa. The size of the red circle indicates the contribution to the phonon linewidth.

To examine the superconducting properties of ScH₁₂ and ScH₁₃, we calculated the logarithmic average phonon frequency (ω_{\log}), EPC parameter (λ), and Eliashberg phonon spectral function [$\alpha^2F(\omega)$] at 300 GPa. As shown in Fig. 4(a), the vibrational frequencies of the Sc atoms in ScH₁₂ are below 480 cm⁻¹, which contribute 16.3% to the total λ . Meanwhile, the vibrational modes above 480 cm⁻¹ attribute primarily to H atoms and constitute 83.7% of the total λ . For ScH₁₃, the phonon spectrum are divided into three regions [Fig. 4 (b)], low frequency modes from Sc (below 430 cm⁻¹, 15.7% of total λ), medium frequency modes from H and H₂ (430-2300 cm⁻¹, 77.1% of total λ),

and high frequency vibrations of quasi-molecular H₂ (only 7.2% of total λ). For ScH₁₂, the calculated EPC parameter λ in its dynamic stable pressure range is greater than 2.0, suggesting very strong EPC. The λ in ScH₁₂ shows a decreasing trend upon increasing the pressure, having the maximum value of 4.24 at 90 GPa, and the minimum 2.5 at 300 GPa. Using typical Coulomb pseudopotential μ^* (0.1-0.13), application of the Eliashberg equations yields a very high T_c value ranging 304-325 K for ScH₁₂ at 300 GPa (Fig. S10, Table S3). This qualifies ScH₁₂ as potentially a room temperature superconductor. Strikingly, as shown in Fig. 5, the superconductivity of ScH₁₂ is weakly pressure dependent, maintaining room temperature superconductivity to a significantly lower pressure of 90 GPa compared to other compressed hydrides (e.g. YH₁₀ at 250 GPa, Li₂MgH₁₆ at 250 GPa). In the case of ScH₁₃, the highest T_c is calculated to be 185 K ($\mu^* = 0.1$) at 300 GPa with $\lambda = 1.40$ and $\omega_{\log} = 1404.3$ K, which is much lower than that of ScH₁₂. Upon decreasing the pressure, the λ in ScH₁₃ initially decreases and then increases, and reaches the maximum value of 1.81 at 90 GPa. Both T_c and ω_{\log} of ScH₁₃ decrease with pressure.

The room-temperature superconductivity predicted in ScH₁₂ prompt us to investigate the isostructural MH₁₂ and MH₁₃ with other metal elements. Using similar Pauling electronegativity (~ 1.3) and atomic radius (~ 1.6 Å) as the criteria, we found Mg, Zr, Hf and Lu. Subsequent calculations of phonon dispersion relations confirm that the corresponding MH₁₂ and MH₁₃ of these four metals are dynamically stable (Figs. S11-S12). In comparison, MH₁₂ and MH₁₃ hydrides with Ca, Y, La, Ac and Th are dynamically unstable up to at least 600 GPa, due to large atomic radius or low electronegativity. The thermodynamic stability of MH₁₂ and MH₁₃ is determined in their corresponding convex hulls (Figs. S13-16) established by structures of all M-H stoichiometries, which are obtained in extensive random structure search. With the ZPE accounted, MgH₁₂ and HfH₁₂ are very close to the convex hull (1~4 meV/atom), while ZrH₁₂ and LuH₁₂ are slightly higher above (14-15 meV/atom), at 300 GPa. These metastable structures are still energetically favorable with respect to the starting material (MH₃ + H₂) and likely to be synthesized under high-pressure high-temperature

conditions.

As shown in Fig. 5, MH_{12} ($\text{M} = \text{Mg}, \text{Zr}, \text{Hf}, \text{and Lu}$) are also calculated to have room temperature T_c between 333 K and 398 K (using $\mu^* = 0.10$). Remarkably, MgH_{12} has a predicted T_c of 376 K at 210 GPa. We note that during the preparation of this manuscript, the same cubic structure of MgH_{12} with high T_c of 402 K at 500 GPa was first reported by Shipley *et al.*³⁵ However, the structure was not discussed in depth, since the focus was on high-throughput screening of high- T_c superconductors. All of predicted MH_{12} hydrides in the present work possess extraordinarily high T_c similar to atomic metallic hydrogen (~ 356 K at 500 GPa³⁶). Likewise, MH_{13} hydrides, namely MgH_{13} , ZrH_{13} , HfH_{13} and LuH_{13} , also host high T_c with 324 K at 300 GPa, 204 K at 400 GPa, 211 K at 450 GPa and 164 K at 100 GPa, respectively. In the case of MH_{13} , the phonon modes associated with the wagging of quasi-molecular H_2 and the vibrations of the metal are primarily responsible for the EPC, while the high-frequency vibrations of H_2 have minor contribution ($< 10\%$). Comparing the H-H distances in MH_{12} and MH_{13} , the nearest H-H distances in ZrH_{12} , HfH_{12} and LuH_{12} are comparable to that in atomic hydrogen solid (Fig. S17). ELF and COHP analysis (Figs. S18-S29), along with the H-H bond lengths, confirm that the hydrogen in MH_{12} and MH_{13} are arranged in quasi-atomic H_2 and quasi-molecular H_2 , respectively. As such, the ELF value and the nearest H-H distance have an approximately linear correspondence (Fig. S30).

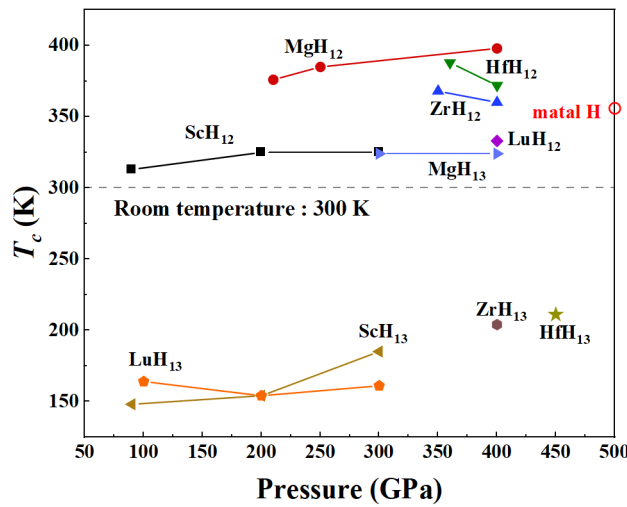


Fig. 5. Pressure dependence of T_c . Calculated T_c of MH_{12} and MH_{13} ($\text{M} = \text{Sc}, \text{Mg}, \text{Zr}, \text{Hf}, \text{Lu}$) by numerically solving Eliashberg equations at different pressures with $\mu^* =$

0.10.

The electronic band structures and project DOS of MH_{12} and MH_{13} are shown in Figs. S31-S34. Given the uniqueness of magnesium superhydrides, we first discuss other $\text{MH}_{12, 13}$ ($\text{M} = \text{Sc}, \text{Zr}, \text{Hf}, \text{Lu}$). A common feature displayed in MH_{12} is the van Hove singularity with a large total DOS value near the Fermi level, formed by strong hybridization of d -orbital (f -orbital) of metal atoms and the s -orbital of H atoms. In contrast, the DOS in MH_{13} is essentially flat around the Fermi level. Thus, the van Hove singularity plays an important role in enhancing the EPC and increasing T_c in MH_{12} . This mechanism is seen in other high- T_c superconductors such as H_3S and LaH_{10} . The comparison of MH_{12} to H_3S and LaH_{10} at 300 GPa (Fig. S35) shows that MH_{12} has a significantly larger DOS at the Fermi level, with a trend $\text{MH}_{12} > \text{LaH}_{10} > \text{MH}_{13} > \text{H}_3\text{S}$. Neither MgH_{12} nor MgH_{13} displays van Hove singularity near the Fermi level, since the d -state of Mg is almost empty in the valence bands (Fig. S36). But, in MgH_{12} and MgH_{13} the electrons transferred to the H atoms significantly enhance the DOS of H ($\sim 86\%$), a scenario also occurred in MgH_6 ³⁷. As shown in Fig. S37, the band structures of MgH_{12} and MgH_{13} are highly resemble to Mg_0H_{12} and Mg_0H_{13} (hypothetical structures with Mg removed from the hydrides), exhibiting a pure hydrogen character. The presence of Mg provides electrons to the H_2 units, which weakens the H-H bonds and stabilizes the structure through ionic Mg-H interaction. MgH_{12} and MgH_{13} are therefore a notable case for achieving metallization and room-temperature superconductivity in hydrides at much lower pressure compared to pure hydrogen.

In summary, extensive structure search combined with *ab initio* calculations reveals a unique superhydride MH_{12} ($\text{M} = \text{Sc}, \text{Mg}, \text{Zr}, \text{Hf}, \text{Lu}$) under high pressure. In this structure, hydrogen atoms are arranged in quasi-atomic H_2 units, which is very different from the hydrogen configurations in known high- T_c hydrides H_3S and LaH_{10} . MH_{12} is calculated to have superconducting critical temperature T_c similar or even superior to metallic hydrogen solids, exhibiting superconductivity at the highest temperature among all known/predicted binary hydrides. Significantly, the calculated T_c of ScH_{12} is 297-313 K at 90 GPa, which realizes room temperature superconductivity at pressures

below one megabar. In MH_{13} , hydrogen atoms form quasi-molecular H_2 units in addition to an isolated H atom, which is also predicted to possess high T_c . The present results provide a prediction of superconductivity in binary hydrides near room temperature. The remarkable T_c s predicted in this work will stimulate high-pressure experimental studies in the future.

Acknowledgements

This work was supported by the National Key Research and Development Program of China (No. 2018YFA0305900 and No. 2022YFA1402304), the National Natural Science Foundation of China (Grants No. 12122405, No. 52072188, No. 12274169, and No. 51632002), the Natural Sciences and Engineering Research Council of Canada (NSERC), program for Changjiang Scholars and Innovative Research Team in University (Grant No. IRT_15R23), and Jilin Provincial Science and Technology Development Project (20210509038RQ). Some of the calculations were performed at the High Performance Computing Center of Jilin University and using TianHe-1(A) at the National Supercomputer Center in Tianjin

Competing interests

The authors declare no competing interests.

References

- 1 Wigner, E. & Huntington, H. B. On the possibility of a metallic modification of hydrogen. *J. Chem. Phys.* **3**, 764-770, (1935).
- 2 Ashcroft, N. W. Metallic Hydrogen: A High-Temperature Superconductor? *Phys. Rev. Lett.* **21**, 1748-1749, (1968).
- 3 Dalladay-Simpson, P., Howie, R. T. & Gregoryanz, E. Evidence for a new phase of dense hydrogen above 325 gigapascals. *Nature* **529**, 63-67, (2016).
- 4 Loubeyre, P., Occelli, F. & Dumas, P. Synchrotron infrared spectroscopic evidence of the probable transition to metal hydrogen. *Nature* **577**, 631-635, (2020).
- 5 Ashcroft, N. W. Hydrogen dominant metallic alloys: high temperature superconductors? *Phys. Rev. Lett.* **92**, 187002, (2004).
- 6 Duan, D. *et al.* Structure and superconductivity of hydrides at high pressures. *Natl. Sci. Rev.* **4**, 121-135, (2017).
- 7 Flores-Livas, J. A. *et al.* A perspective on conventional high-temperature superconductors at high pressure: Methods and materials. *Phys. Rep.-Rev. Sec. Phys. Lett.* **856**, 1-78, (2020).
- 8 Pickard, C. J. & Needs, R. J. Structure of phase III of solid hydrogen. *Nat. Phys.* **3**, 473-476, (2007).
- 9 Loubeyre, P. *et al.* X-ray diffraction and equation of state of hydrogen at megabar pressures. *Nature* **383**, 702-704, (1996).
- 10 Mao, H.-k. & Hemley, R. J. Ultrahigh-pressure transitions in solid hydrogen. *Rev. Mod. Phys.* **66**, 671-692, (1994).
- 11 Li, Y. *et al.* Superconductivity at approximately 100 K in dense $\text{SiH}_4(\text{H}_2)_2$ predicted by first principles. *Proc. Natl. Acad. Sci. U. S. A.* **107**, 15708-15711, (2010).
- 12 Zhong, X. *et al.* Tellurium Hydrides at High Pressures: High-Temperature Superconductors. *Phys. Rev. Lett.* **116**, 057002, (2016).
- 13 Duan, D. *et al.* Pressure-induced metallization of dense $(\text{H}_2\text{S})_2\text{H}_2$ with high- T_c superconductivity. *Sci. Rep.* **4**, 6968, (2014).
- 14 Duan, D. F. *et al.* Pressure-induced decomposition of solid hydrogen sulfide. *Phys. Rev. B* **91**, (2015).
- 15 Drozdov, A. P., Eremets, M. I., Troyan, I. A., Ksenofontov, V. & Shylin, S. I. Conventional superconductivity at 203 kelvin at high pressures in the sulfur hydride system. *Nature* **525**, 73-76, (2015).
- 16 Einaga, M. *et al.* Crystal Structure of the Superconducting Phase of Sulfur Hydride. *Nat. Phys.* **12**, 835-838, (2016).
- 17 Peng, F. *et al.* Hydrogen Clathrate Structures in Rare Earth Hydrides at High Pressures: Possible Route to Room-Temperature Superconductivity. *Phys. Rev. Lett.* **119**, 107001, (2017).
- 18 Liu, H., Naumov, I., Hoffmann, R., Ashcroft, N. W. & Hemley, R. J. Potential high- T_c superconducting lanthanum and yttrium hydrides at high pressure. *Proc. Natl. Acad. Sci. U. S. A.* **114**, 6990-6995, (2017).

- 19 Geballe, Z. M. *et al.* Synthesis and Stability of Lanthanum Superhydrides. *Angew. Chem.-Int. Edit.* **57**, 688-692, (2018).
- 20 Drozdov, A. P. *et al.* Superconductivity at 250 K in lanthanum hydride under high pressures. *Nature* **569**, 528-531, (2019).
- 21 Somayazulu, M. *et al.* Evidence for Superconductivity above 260 K in Lanthanum Superhydride at Megabar Pressures. *Phys. Rev. Lett.* **122**, 027001, (2019).
- 22 Hong, F. *et al.* Superconductivity of Lanthanum Superhydride Investigated Using the Standard Four-Probe Configuration under High Pressures. *Chin. Phys. Lett.* **37**, (2020).
- 23 Xie, H. *et al.* Hydrogen Pentagraphenelike Structure Stabilized by Hafnium: A High-Temperature Conventional Superconductor. *Phys. Rev. Lett.* **125**, 217001, (2020).
- 24 Sun, Y., Lv, J., Xie, Y., Liu, H. & Ma, Y. Route to a Superconducting Phase above Room Temperature in Electron-Doped Hydride Compounds under High Pressure. *Phys. Rev. Lett.* **123**, 097001, (2019).
- 25 Xiao, H., Dan, Y., Suo, B. & Chen, X. Comment on “Accelerated Discovery of New 8-Electron Half-Heusler Compounds as Promising Energy and Topological Quantum Materials”. *J. Phys. Chem. C* **124**, 2247-2249, (2020).
- 26 Zhou, D. *et al.* Superconducting praseodymium superhydrides. *Sci. Adv.* **6**, eaax6849, (2020).
- 27 Mishra, A. K. *et al.* New Calcium Hydrides with Mixed Atomic and Molecular Hydrogen. *J. Phys. Chem. C* **122**, 19370-19378, (2018).
- 28 Pickard, C. J. & Needs, R. J. Ab initio random structure searching. *J. Phys.-Condes. Matter* **23**, 053201, (2011).
- 29 Ye, X., Zarifi, N., Zurek, E., Hoffmann, R. & Ashcroft, N. W. High Hydrides of Scandium under Pressure: Potential Superconductors. *J. Phys. Chem. C* **122**, 6298-6309, (2018).
- 30 Testardi, L. R. Structural instability and superconductivity in A-15 compounds. *Rev. Mod. Phys.* **47**, 637-648, (1975).
- 31 Szczeniak, R. & Durajski, A. P. Superconducting state above the boiling point of liquid nitrogen in the GaH₃ compound. *Supercond. Sci. Technol.* **27**, (2014).
- 32 Abe, K. & Ashcroft, N. W. Quantum disproportionation: The high hydrides at elevated pressures. *Phys. Rev. B* **88**, (2013).
- 33 Shao, Z. J. *et al.* Ternary superconducting cophosphorus hydrides stabilized via lithium. *npj Comput. Mater.* **5**, 1-8, (2019).
- 34 Pickard, C. J., Martinez-Canales, M. & Needs, R. J. Density functional theory study of phase IV of solid hydrogen. *Phys. Rev. B* **85**, (2012).
- 35 Shipley, A. M., Hutcheon, M. J., Needs, R. J. & Pickard, C. J. High-throughput discovery of high-temperature conventional superconductors. *Phys. Rev. B* **104**, (2021).
- 36 McMahon, J. M. & Ceperley, D. M. High-temperature superconductivity in atomic metallic hydrogen. *Phys. Rev. B* **84**, (2011).
- 37 Feng, X., Zhang, J., Gao, G., Liu, H. & Wang, H. Compressed sodalite-like

MgH₆ as a potential high-temperature superconductor. *RSC Adv.* **5**, 59292-59296, (2015).